

Empirical Nusselt Number Correlation for Single Phase Flow through a Plate Heat Exchanger

ALI HASHMI, FRAAZ TAHIR, UMAIR HAMEED

Faculty of Mechanical Engineering
Ghulam Ishaq Khan Institute (GIKI)
Topi (23640), Khyber Pakhtunkhwa
PAKISTAN
hashmiii.ali@gmail.com

Abstract: - The objective of the study is to investigate the heat transfer characteristics and thermal performance of a plate heat exchanger. An experimental setup at the Natural Fluids Refrigeration Centre (NFRC), GIKI was used to develop an empirical correlation to estimate single-phase heat transfer for a plate heat exchanger with a specified configuration of commercially available chevron plates. Experiments were conducted using water at various flow rates and temperatures in order to develop a correlation via modified Wilson plot technique corresponding to a maximum Reynolds number (Re) of 4500 and Prandtl number (Pr) in the range of 5.6 to 8.

Key-Words: - Plate heat exchanger, Single phase, Nusselt number, Chevron plates, Modified Wilson plot

1 Introduction

Plate Heat Exchangers (PHE) are widely used in dairy, pharmaceutical and paper industry as well as in HVAC applications due to numerous advantages. A number of analytical and experimental studies have been conducted to study the heat transfer characteristics of tubular heat exchangers. However, a very limited work is found in open literature regarding heat transfer through plate heat exchangers. Owing to commercial non-disclosure, there is a scarcity of design information pertaining to plate heat exchangers.

Most of the available single-phase heat transfer correlations for plate heat exchangers are geometry specific and are applicable within a certain range of Reynolds and Prandtl numbers. Problem arises since majority of previous studies provide incomplete information about the operating conditions and the plate geometry. For industrial and practical applications, it is imperative that Nusselt number correlations with complete information are available.

The objective of this study was to investigate the thermal performance of a commercially available plate heat exchanger with a mixed plate configuration. The effect of cold side Reynolds number on the Nusselt number correlation, for a fixed cold side Prandtl number was investigated. Experiments were conducted and a correlation was developed using modified Wilson plot technique. The presented correlation was then compared with those developed by other researchers.

2 Modified Wilson Plot

Generally, for single-phase heat transfer, Nusselt number correlation is represented by an empirical expression of the form:

$$Nu = C * Re^p Pr^n \left(\frac{\mu}{\mu_s} \right)^{0.14} \quad (1)$$

'Nu' in the expression above on the left hand side represents the Nusselt number. 'C', 'p', and 'n' in (1) are constants independent of the nature of fluid used. The last term in the expression on the right hand side of the equality accounts for the variable viscosity effect. [1]

'Nu' is also equivalent to:

$$Nu = \frac{h * D_h}{k_f}$$

Where: h is the convective heat transfer coefficient, D_h , is the hydraulic diameter and k_f , is the thermal conductivity of the fluid.

Modified Wilson plot technique is primarily used to determine the value of multiplier 'C' and exponent of Reynolds number 'p' in the Nusselt number correlation [2]. The magnitude of 'n' is taken to be 1/3 in agreement with [3] and [4]. The following basic relation (2) is algebraically manipulated in two different ways to obtain equations (3) and (4), which are subsequently used for obtaining the modified Wilson plot [5].

$$\frac{1}{U} = \frac{1}{h_h} + \left(\frac{t}{k}\right)_{wall} + \frac{1}{h_c} \quad (2)$$

The subscripts ‘c’ and ‘h’ indicate the cold and hot fluids.

The first modification yields equation (3) which is of the linear form:

$$Y_1 = mX_1 + b \quad (3)$$

Where:

$$Y_1 = \left(\frac{1}{U} - \frac{t}{k_{wall}}\right) \left[\frac{k_c}{D_{hyd}} \text{Re}_c^p \text{Pr}_c^{\frac{1}{3}} \left(\frac{\mu}{\mu_s}\right)_c^{0.14} \right]$$

$$X_1 = \frac{\frac{k_c}{D_{hyd}} \text{Re}_c^p \text{Pr}_c^{\frac{1}{3}} \left(\frac{\mu}{\mu_s}\right)_c^{0.14}}{\frac{k_h}{D_{hyd}} \text{Re}_h^p \text{Pr}_h^{\frac{1}{3}} \left(\frac{\mu}{\mu_s}\right)_h^{0.14}}$$

$$\text{Gradient: } m = \frac{1}{C_h}$$

and,

$$\text{Intercept: } b = \frac{1}{C_c}$$

An initial guess ‘p’ is used to obtain a plot between X_1 and Y_1 , which yields C_c and C_h .

Given below is the second algebraic modification of (2):

$$\left(\frac{1}{U} - \frac{t}{k_{wall}} - \frac{1}{h_h}\right) * \left[\text{Pr}_c^{\frac{1}{3}} \left(\frac{\mu}{\mu_s}\right)_c^{0.14} \frac{k_c}{D_{hyd}}\right] = \frac{1}{C_c \text{Re}_c^p}$$

$$y_2 = \frac{1}{(C_c \text{Re}_c^p)}$$

$$\ln y_2 = -\ln C_c - p \ln \text{Re}_c \quad (4)$$

The equation (4) above is also of the linear form

$$Y_2 = mX_2 + b$$

Where:

$$m = -p, \quad b = -\ln C_c$$

The value of C_h obtained from the linear plot (X_1, Y_1) coupled with the initial guess value of ‘p’ is used to obtain a second plot (X_2, Y_2) as delineated by (4). The absolute value of the gradient of second plot is the new value of ‘p’. This value is reinserted into (3) to acquire yet another value, which converges to the root with subsequent iterations. The procedure is repeated until the difference between consecutive values of the gradient reaches a value smaller than the prescribed error.

3 Experimentation

3.1 Experimental setup

A schematic of the experimental apparatus is shown in Fig.1. The central piece of equipment is the plate heat exchanger. The setup consists of a hot fluid loop and a cold fluid loop. The hot fluid loop consists of a hot fluid tank and a pump that forces hot fluid from the tank to the heat exchanger. The hot fluid tank has a capacity of

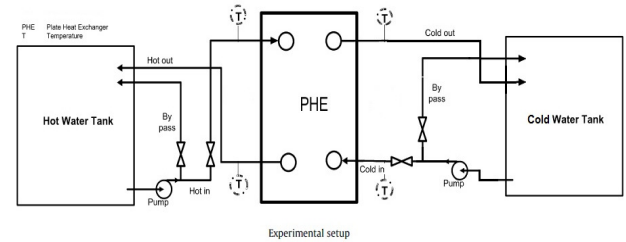


Fig.1: Schematic of the experimental apparatus

150 US gallons and is equipped with six electric immersion heaters. One of the heaters is attached to a temperature controller and magnetic contactor. The cold fluid loop consists of a tank and a pump that forces cold fluid from the tank to the heat exchanger. The cold fluid tank has a capacity of 35 US gallons. Temperatures are measured at the inlet and exit of the plate heat exchanger for both the hot and the cold fluid streams using the Resistance Temperature Detectors (RTDs). The fluid is cooled by a 2 TR Packaged Air Cooled Water Chiller. The side walls of the heat exchanger, water tank and piping were well insulated with polyurethane foam, covered with aluminum foil, to minimize any loss or gain of heat.

When the desired temperature settings of the cold and hot fluids were achieved, the fluids of both the loops were pumped into the Plate heat exchanger, where they exchanged heat. The hot fluid flowed

from top to bottom within a channel of the plate heat exchanger while the cold fluid flowed from bottom to the top of the channel achieving counter-flow. Experiments were conducted at various temperatures and flow rates of hot and cold fluids using plates of a fixed chevron angle, $\beta = 45^\circ$. Such plate configuration was achieved using a combination of 30° and 60° plates.

Reynolds number was varied by changing the fluid flow rate through a variable frequency drive and bypass valves. Prandtl number was varied by changing the temperature of the fluid using chiller, heaters and temperature controllers. The desired temperature of water at the inlet of the plate heat exchanger, PHE, was controlled to an accuracy of $\pm 0.1^\circ\text{C}$. The system was allowed to reach the steady state before any reading was made.

3.1.1 Heat Exchanger Specifications

A commercial gasketed plate heat exchanger was used for this study. Important geometric characteristics of a chevron plate as defined by Kakac et al. [6] are shown in Fig.2. Geometric parameters are defined in Table 1, similar to the descriptions of Ayub [7]. Geometric details of the chevron plates used for the experimentation are provided in Table 2. The plate heat exchanger was configured in a single pass, U-arrangement, allowing ease of disassembly. In a U-arrangement, all inlet/exit ports for both fluid streams are on the same fixed plate side, permitting counter-flow mechanism for the two fluid streams.

Fig.2: Geometric characteristics of chevron plate

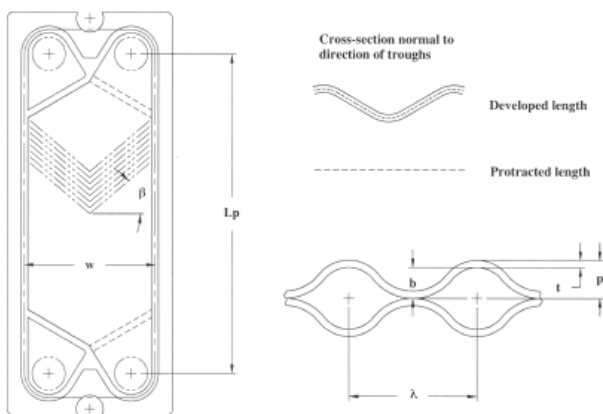


Table 1: Important geometric characteristics of chevron plate

Chevron angle, β	Usually termed β and varies between $22^\circ - 65^\circ$
------------------------	---

Mean Flow Channel Gap, b	This is defined as the actual gap available for the flow: $b = p - t$
Surface enlargement factor, ϕ	This factor is the ratio of the developed length to the protracted length
Channel flow area, A_x	This is the actual flow area defined as: $A_x = b \cdot w$
Channel hydraulic diameter, D_h	D_h is defined as four times ratio of minimum flow area to wetted perimeter: $D_h = 2b/\phi$ [8]

Table 2: Geometric characteristics of chevron plate used in this study

Plate width (mm)	w	185
Vertical distance b/w ports (mm)	L_p	565
Channel spacing (mm)	b	2.2
Effective area (m^2)	A_x	0.095
Plate thickness (mm)	t	0.5
Surface enlargement factor	ϕ	1.117
Chevron angle	β	45°

3.1.2 Instrumentation

The experimentation required temperatures ranging from 12°C to 32°C . The terminal temperatures were measured by three wire Pt-100 resistance temperature detectors (RTDs) of mineral insulated stainless steel sheathed class "A" with measurement uncertainty of $\pm 0.1^\circ\text{C}$. These RTDs have a sheath diameter of 6 mm and length of 100 mm, provide stable output for long period with high accuracy, and are easy to recalibrate. Nine RTDs were calibrated relative to a reference RTD. The selected reference was a brand new, factory calibrated RTD. The RTDs were installed at all four ports of the plate heat exchanger, in well-insulated pipe sections, to measure the temperatures of both fluids. The data logger used was a 16-channel input device with an LCD display and graphic representation of the data.

3.2 Experimental Procedure

The variable speed water pump was switched on, in order to start the hot water circulation. The cold-water circulation was then started by switching on the cold-water pump. A chiller was used to maintain the desired cold-water temperature. The heating of hot water side was initiated by switching on the desired number of submerged water heaters in the

hot water tank. The tank was provided with six submerged heating elements, ranging from 1-3 kW. The number of heaters used was dependent on the heat flux required for a specific experiment. One of the heaters was connected to the hot water inlet RTD through an on/off switch and a digital thermostat, which was capable of controlling the temperature within $\pm 0.1^\circ\text{C}$. The hot water inlet temperature, set using a thermostat, was pre-selected based on the desired value of Prandtl number. The hot water flow rate was adjusted by means of a power inverter. The cold-water flow rate was adjusted to the desired Reynolds number settings by the flow control valve. Flow rate measurements were taken by the conventional bucket and stopwatch method. The experiments were conducted in a matrix of varying cold side Reynolds number at a fixed cold side Prandtl number. Five different Reynolds numbers were used for the Prandtl number setting. Sufficient time was given to the system to achieve steady state condition. The flow rates, temperatures at all inlets and exits of the plate heat exchanger and energy balance were monitored. The goal of the experimentation was to determine the overall heat transfer coefficient, 'U'.

4 Data Reduction

The primary measurements recorded were fluid flow rates, and temperatures at inlet and exit of the plate heat exchanger for both the fluids. Property tables for water were incorporated into a custom-built MATLAB program for the ease of interpolation and calculation of the fluid properties. The values of the measured flow rates and temperatures were input to the Graphical User Interface (GUI) of the program, which provided fluid properties at the bulk mean fluid temperatures given below:

$$T_{c,avg} = \left(\frac{T_{c,i} + T_{c,o}}{2} \right) \quad (5)$$

$$T_{h,avg} = \left(\frac{T_{h,i} + T_{h,o}}{2} \right) \quad (6)$$

Where, the subscripts 'c' and 'h' indicate the cold and hot fluids, and 'i' and 'o' represent the inlet and the outlet fluid streams respectively.

Mass flow rate of the cold and hot fluid stream was calculated using density of water evaluated at the respective bulk mean temperatures (5) and (6).

The wall temperature (7) at which viscosity was evaluated was the average of the cold and hot fluid temperatures at both the inlets and the outlets.

$$T_{wall} = \left(\frac{T_{c,i} + T_{c,o} + T_{h,i} + T_{h,o}}{4} \right) \quad (7)$$

The overall heat transfer coefficient, U, was determined as follows by (8):

$$U = \frac{Q_{avg}}{A * \Delta T_{LMTD}} \quad (8)$$

' Q_{avg} ' is the average of the rate of heat transfer, 'A' is the effective heat transfer surface area and ΔT_{LMTD} is the log-mean temperature difference for counter flow arrangement, given by (9):

$$\Delta T_{LMTD} = \left\{ \frac{(T_{h,i} - T_{c,o}) - (T_{h,o} - T_{c,i})}{\ln \left[\frac{(T_{h,i} - T_{c,o})}{(T_{h,o} - T_{c,i})} \right]} \right\} \quad (9)$$

The rate of heat transfer (10) was calculated at steady state condition using energy balance:

$$Q = m * C_p * \Delta T \quad (10)$$

Where, ΔT is the difference in fluid temperatures between inlet and outlet conditions and C_p is the specific heat at constant pressure and m is the mass flow rate.

The difference between the rate of heat transfer on hot and cold sides was within $\pm 5\%$.

The Reynolds and Prandtl numbers are determined from the fluid properties found at the bulk mean fluid temperatures. These dimensionless numbers along with the overall heat transfer coefficient, U, are then used for the analysis.

5 Results and Discussion

After gathering adequate experimental data, modified Wilson plots were generated in MATLAB and Microsoft Excel, as shown in Fig.3 and Fig.4.

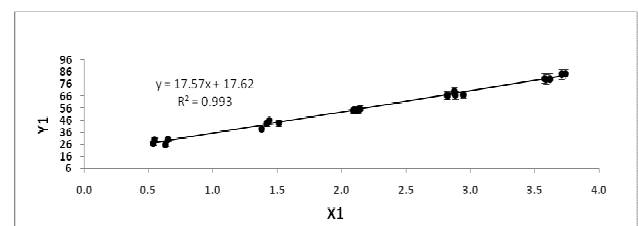
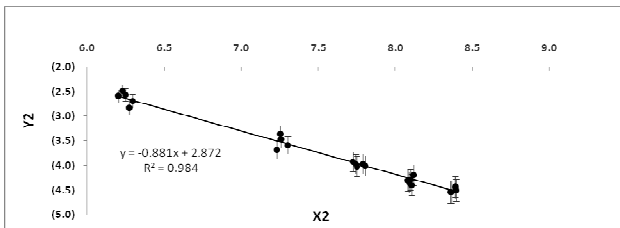


Fig.3: Linear plot (X₁, Y₁)

Fig.4: Logarithmic plot (X_2 , Y_2)

After successive iterations, the gradient and intercept of Fig.4 were found to be:

$$m = 0.881$$

$$C_c = C_h = 0.0566$$

Hence, the Nusselt number correlation is as follows:

$$Nu = 0.0566 Re^{0.881} Pr^{\frac{1}{3} \left(\frac{\mu}{\mu_s} \right)^{0.14}} \quad (11)$$

The abovementioned empirical correlation is valid for following range of experimentation and plate configuration:

$$500 < Re < 4500$$

$$5.6 < Pr < 8.0$$

$$\text{Chevron angle } (\beta) = 45^\circ$$

The correlation was compared with those of other researchers conforming to the range of experimentation and configuration used for the present study. The results in Fig. 5 show that the correlation is comparable to those of Khan [9], Thonon [10], and Cooper [11]. The correlation is also a strong function of the Reynolds number; a similar trend has also been observed by Warnakulasuriya and Worek [12].

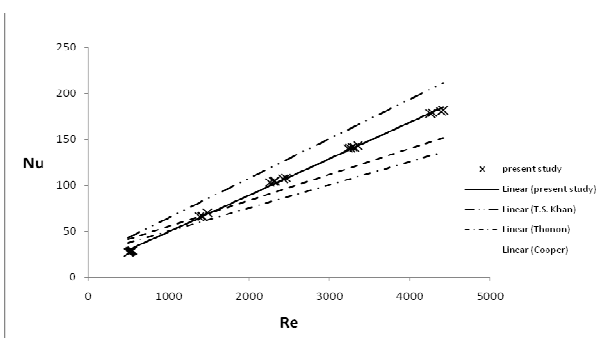


Fig.5: Nusselt vs. Reynolds comparison

Since the modified Wilson plot technique used earlier for the analysis comprised of an iterative interplay between two equations, (3) and (4), therefore, only two unknowns could be

estimated: ' C ' and ' m ' for the present study. The exponent of Prandtl number ' n ' had to be known initially, and it was taken to be 1/3. The reason for this assumption was that most of the empirical correlations developed in the past have agreed to a value for the Prandtl number's exponent to lie in the range between 0.3 and 0.4. After the correlation was developed, it was felt necessary to investigate the effect of varying the value of ' n ' on the form of the correlation. Arbitrary values were assigned to the Prandtl number's exponent, and analysis was carried out several times to note for any changes occurring in the form of the Nusselt number correlation.

Table 3 below demonstrates the effect of varying the exponent ' n ' of the Prandtl number on the multiplier ' C ' and exponent ' m ' in the Nusselt number correlation.

n	C	m
0.30	0.060	0.882
0.33	0.057	0.881
0.35	0.055	0.881
0.40	0.049	0.883

Table 3: Effect of ' n ' on ' C ' and ' m '

It was found that varying the exponent of Prandtl number had negligible effect on the Nusselt number itself. Thus, the empirical correlation (11) showed a weak dependence on Prandtl number's exponent.

6 Conclusion

Experiments were performed to investigate the thermal performance of a commercial plate heat exchanger with mixed plate configuration by developing an empirical single-phase heat transfer correlation. It was found that the Nusselt number correlations for the hot and cold sides are the same because the multipliers in the correlation (i.e. C_c and C_h) were equal. Although experimentation was performed with a fixed cold side Prandtl number, the above result means that the correlation is valid for an extended range of Prandtl numbers. The presented correlation is applicable for $500 < Re < 4500$ and $5.6 < Pr < 8.0$ with $\beta = 45^\circ$.

Nusselt number was found to be a strong function of Reynolds number. In contrast, changing the value of the Prandtl number's exponent ' n ' in the correlation

while keeping all other terms constant had negligible effect on Nusselt number. Thus, a value of 1/3 for the Prandtl number's exponent used in accordance with the earlier research is justified.

Acknowledgement

The authors appreciate the cooperation of the faculty at the Ghulam Ishaq Khan Institute and particularly the practical assistance provided by staff at Natural Fluids Refrigeration Centre (NFRC).

References:

- [1] X1. F. P. Incropera, *Fundamentals of Heat and Mass transfer 5th edition*, John Wiley & Sons, 2001.
- [2] X2. J. Fernandez-Seara, F. J. Uhiá, J. Sieres, A. Campo, A General Review of the Wilson Plot Method and its Modifications to Determine Convection Coefficients in Heat Exchange Devices, *Applied Thermal Engineering*, Vol. 27, 2007, pp. 2745–2757.
- [3] X3. M. F. Edwards, A. A. Chngal Vaie and D. L. Parrott, Heat Transfer and Pressure Drop Characteristics of a Plate Heat Exchanger Using Non-Newtonian Liquids, *The Chemical Engineer*, no. 285, 1974, pp. 286–288, 293,.
- [4] X4. A. Muley and R. M. Manglik, Experimental Study of Turbulent Flow Heat Transfer and Pressure Drop in a Plate Heat Exchanger with Chevron Plates, *Journal of Heat Transfer*, vol. 121, no. 1, 1999, pp. 110–117.
- [5] X5. J. Pettersen, R. Rieberer, S. Tollak, Heat Transfer and Pressure Drop for Flow of Supercritical and Subcritical CO₂ in Microchannel Tubes, February 2000.
- [6] X6. S. Kakac, S. Liu, *Heat Exchangers Selection, Rating and Thermal Design*, CRC, USA, 2002 (Chapter 10).
- [7] X7. Z.H. Ayub, Plate heat exchanger literature survey and new heat transfer and pressure drop correlations for refrigerant evaporators, *Heat Transfer Engineering*, 24, 2003, pp. 3–16.
- [8] X8. R.L. Heavner, H. Kumar, A.S. Wanniarachchi, Performance of an industrial heat exchanger: effect of chevron angle, *AIChE Symposium Series*, vol. 89, no. 295, New York, 1993, pp. 262–267.
- [9] X9. T.S. Khan, M.S. Khan, Ming-C. Chyu, Z.H. Ayub, Experimental investigation of single phase convective heat transfer coefficient in a corrugated plate heat exchanger for multiple plate configurations, *Applied Thermal Engineering*, 30, 2010, pp. 1058–1065.
- [10] X10. B. Thonon, Design method for plate evaporators and condensers, in: 1st International Conference on Process Intensification for the Chemical Industry, *BHR Group Conference Series Publication*, 18, 1995, pp. 37–47.
- [11] X11. A. Cooper, Recover More Heat with Plate Heat Exchangers, *The Chemical Engineer*, no. 285, 1974, pp. 280–285.
- [12] X12. F.S.K. Warnakulasuriya, W.M. Worek, Heat transfer and pressure drop properties of high viscous solutions in plate heat exchangers, *International Journal of Heat and Mass Transfer*, Vol. 51, 2008, pp. 52–67.